



OPEN ACCESS

EDITED BY

Leilei Zhang,
Rice University, United States

REVIEWED BY

Zhengzheng Cao,
Henan Polytechnic University, China
Tian HE,
China University of Petroleum, Beijing, China

*CORRESPONDENCE

Ruidong Zhao,
✉ zhaoruidong@petrochina.com.cn

RECEIVED 28 October 2025

REVISED 04 December 2025

ACCEPTED 29 December 2025

PUBLISHED 13 January 2026

CITATION

Yang J, Zhao R and Ma G (2026) A digital production metering method for electrical submersible pumps wells based on system energy balance.

Front. Earth Sci. 13:1733797.

doi: 10.3389/feart.2025.1733797

COPYRIGHT

© 2026 Yang, Zhao and Ma. This is an open-access article distributed under the terms of the [Creative Commons Attribution License \(CC BY\)](https://creativecommons.org/licenses/by/4.0/). The use, distribution or reproduction in other forums is permitted, provided the original author(s) and the copyright owner(s) are credited and that the original publication in this journal is cited, in accordance with accepted academic practice. No use, distribution or reproduction is permitted which does not comply with these terms.

A digital production metering method for electrical submersible pumps wells based on system energy balance

Jiani Yang, Ruidong Zhao* and Gaoqiang Ma

Research Institute of Petroleum Exploration and Development, Beijing, China

Conventional production metering in Electrical Submersible Pumps (ESPs) wells relies on devices such as surface flowmeters, test separators, and multiplex valves. However, these methods are limited by poor real-time performance and high infrastructure costs. Digital/Virtual Flow Metering (DFM/VFM) has emerged as a promising alternative to conventional methods. However, existing DFM/VFM methods remain immature, often suffering from low accuracy and limited applicability. To address these challenges, this study proposes a digital production metering method based on system energy balance. The proposed model is established based on the energy balance between the motor output and the pump input and incorporates corrections for fluid property variations between surface and downhole conditions. Unlike standard pump performance curves, which are derived from water tests, this study conducted laboratory experiments on an ESP system to characterize the effects of fluid viscosity (10–50 cP) and density (0.8–1.1 g/cm³) on its performance. The experimental data were used to calibrate the motor and pump performance curves, significantly improving its accuracy and applicability. The model was validated against production data from five wells with different displacement rates. The results showed deviations ranging from 0.19 m³/d to under 20 m³/d, indicating good accuracy. This model provides a precise and cost-effective alternative to digital flowmeters. By eliminating the need for surface flowrate metering devices, the method not only reduces capital and operational expenses but also advances the intelligence of field management.

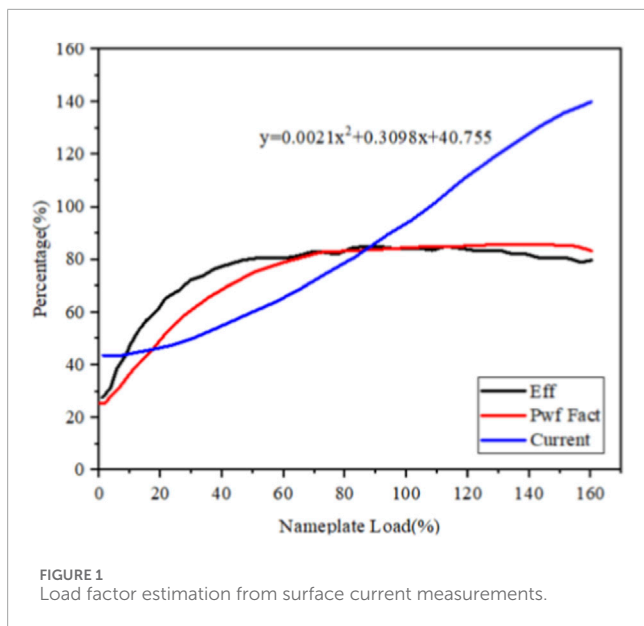
KEYWORDS

digital production calculation, electric submersible pump, laboratory test, mathematical model, performance curve

1 Introduction

Block H oilfield, which is in its mid-to-high water-cut stage, prefers ESPs due to their high displacement and adaptability (Gryzlov et al., 2021). Block H contains 336 ESP wells, with a daily oil production of approximately 1,980.62 tons. However, current production measurement in the block relies primarily on manual methods, which are labor-intensive and lack automation.

In recent years, high-frequency and high-precision digital production measurement has emerged as a prominent research focus. Some scholars (Li et al., 2018; Caicedo and Montoya, 2012; Tangren et al., 1949) have proposed online mathematical models that combine capillary pressure measurement and the principle of energy conservation



with wellbore multiphase flow calculations. To address multiphase flow under complex conditions, the team led by Liu and Chen (2020), Camilleri et al. (2015), Al Qahtani et al. (2020), Amin (2015), Camilleri et al. (2010) proposed a digital production measurement method. Their approach was based on an enhanced Beggs-Brill model. By introducing a gas-phase slippage correction coefficient and dynamically characterizing liquid-phase viscosity, they reduced measurement errors to below 6%.

Similar international studies have focused on throttling equations, including the combined application of Bernoulli’s equation and the fluid continuity equation (Del Pino et al., 2017; Morrison et al., 2014; Camilleri et al., 2016), to calculate flow rates based on pressure differences across chokes. Batzle and Wang (2019), Bismukhametov and Jaschke (2019), Barrios et al. (2012), Varón et al. (2013) established a coupled digital production measurement model for ESP wells in deep formations (>3,000 m), based on classical multiphase fluid mechanics theories. By integrating pump performance curves with wellbore pressure gradient equations, the model achieved an accuracy of ±3% under standard working conditions.

The accurate metering of fluid production in the wellbore is part of the broader challenge of understanding complex fluid evolution in subsurface systems. This broader context includes studies on nonlinear flow and immiscibility in fractured media (Liu and Zhang, 2022), paleofluid migration and slurry diffusion through mining-induced cracks and faults (Reiners et al., 2019), and the energy evolution mechanisms during material failure under dynamic loading (Xue et al., 2024; Peng et al., 2014). Building upon this broader context, this study focuses on production measurement methods for ESP wells without the use of downhole pressure monitoring devices.

This study focuses on production measurement methods for ESP wells without the use of downhole pressure monitoring devices. It utilizes current data, along with experimentally obtained pump and motor performance curves, to develop a mathematical model based

on the energy conservation principle of ESP systems, followed by solving the model.

2 Model establishment

The production rate of the ESP well is calculated using the principle of energy conservation, based on the assumption that the fluid properties remain stable in the short term. Herein, “short term” refers to the interval between two routine manual production tests, which typically ranges from several days to 1 month in the field practice of Block H. To ensure the model’s accuracy over time, an update strategy is employed. Once new production test data becomes available, the model is re-calibrated. This is achieved by recalculating the power discrepancy (ΔP) and updating the P-Q fitting function using the latest data. This process allows the model to adapt to and correct for mid-to-long-term changes in fluid properties. During the production process of an ESP well, electrical energy serves as the power source. Grid voltage transmits electricity to the submersible motor through the submersible power cable. The submersible motor converts electrical energy into mechanical energy, driving the submersible pump to rotate at high speed and lift the well fluid to the surface through the tubing. Throughout this process, the principle of energy conservation is expressed as the input power of the pump equaling the output power of the motor (Equation 1), i.e.:

$$P_{pump} = P_{motor} \tag{1}$$

where P_{pump} is the input power of the pump, kW; P_{motor} is the output power of the motor, kW.

The traditional production estimation model calculates motor output power based on the internal resistance of the cable and motor. In contrast, this approach treats the electric submersible pump system as a series circuit. In such a circuit, the current remains consistent throughout the system. The motor output power is derived by combining surface current data with the motor performance curve—specifically, using the current-load rate curve and the motor’s nameplate rated values to compute P_{motor} (theoretical motor output power = load rate × rated output power). The relationship between surface current and motor load factor is illustrated in Figure 1. As shown in the current curve (green) in Figure 2.

The ESP performance curve includes the following.

- Head (H) vs. Flow Rate (Q),
- Efficiency (η) vs. Flow Rate,
- Power (P) vs. Flow Rate curves.

where power refers to the input power of the submersible pump, i.e., the power transmitted from the submersible motor to the pump shaft. Therefore, P_{pump} can be directly obtained from the P-Q curve in the ESP performance curve.

According to the law of energy conservation, the power values calculated using the motor and pump performance curves should be identical. However, in actual production, due to energy losses such as motor, cable, and pump energy consumption, the motor output power does not correspond to the pump input power. This relationship can be expressed as follows:

$$P_{syse} = P_{hydr} + \Delta P_c + \Delta P_m + \Delta P_p + \Delta P_i \tag{2}$$

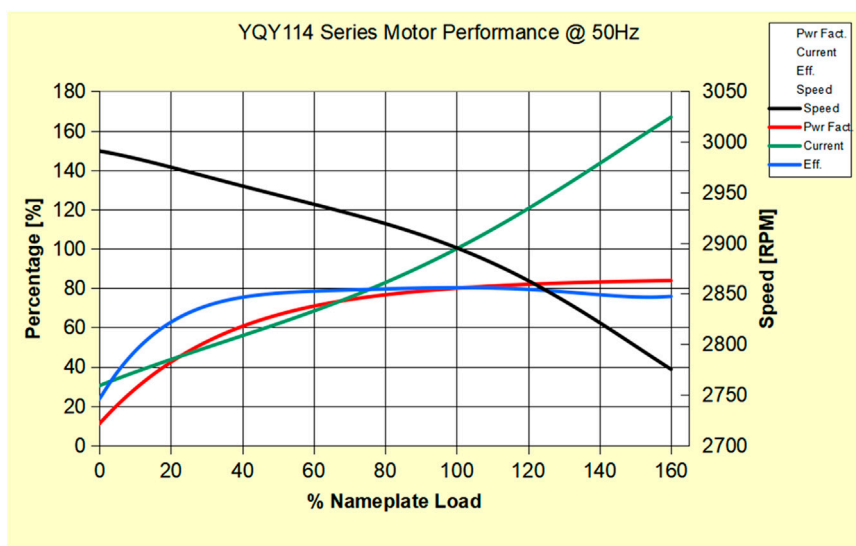


FIGURE 2 Performance curve of YQY95 motor.

TABLE 1 Formation viscosities in Block H.

Formation	Viscosity (cP)
CIII	16.01
CI2 + 3	13.7
CI4 + 5	9.07
CI4	11.18

Where P_{sys} is the system electrical input power; P_{hydr} is power applied to the fluid; ΔP_c is the cable energy consumption; ΔP_m and ΔP_p represent the energy consumption of the electric pump and the motor, respectively; ΔP_i is the protector/separator energy consumption.

Therefore, the difference between the calculated motor input power and the pump output power is considered the total energy loss. This difference is used to correct the original P-Q curve, thus enabling the calculation of the flow rate corresponding to the theoretical motor output power. Additionally, since ESP wells frequently operate with variable frequency drives (VFDs), the impact of frequency variations is accounted for using the affinity laws for electric submersible pumps (Equation 3). This approach directly provides the pump performance curves under actual operating frequencies, eliminating the need for dimensionless processing of the ESP performance curves (Zhou, 2017).

$$\begin{aligned}
 Q_2 &= Q_1 \times (f_2/f_1) \\
 H_2 &= H_1 \times (f_2/f_1)^2 \\
 P_2 &= P_1 \times (f_2/f_1)^3
 \end{aligned}
 \tag{3}$$

Aiming to measure the flow rate for electric submersible pump (ESP) wells without downhole pressure gauges, this research

deviates from the conventional methodology, where the power applied to the fluid is ultimately reflected in the relationship between flow rate and head (i.e., deriving $Q = \frac{P_{motor} - \Delta P_c - \Delta P_m - \Delta P_p - \Delta P_i}{P_d - P_i}$) by combining (Equation 2) with the fundamental equation $P_{hydr} = Q\rho gH = Q(P_d - P_i)$). Instead, it adopts an alternative approach by fitting and correcting the P-Q curve within the pump performance curves to ultimately achieve the goal of production estimation.

Although the experimental study focused on viscosity and density, the model’s applicability extends to scenarios with varying water cuts. This is because changes in water cut primarily affect the bulk fluid viscosity and density. The model inherently accounts for these variations by utilizing the performance curves calibrated for the corresponding effective fluid properties. Therefore, for any given water cut, the effective viscosity and density can be calculated, and the model can employ the corresponding calibrated performance curve, provided the resultant properties fall within the validated range of 10–50 cP and 0.8–1.1 g/cm³. The formation viscosities in Block H, which guided the selection of appropriate performance curves, are listed in Table 1.

3 Acquisition of performance curves

The performance curves of the electric submersible pump (ESP) system, including head (H) vs. flow rate (Q), efficiency (η) vs. flow rate, and power (P) vs. flow rate, are typically obtained through laboratory testing under standardized conditions. These curves are provided by the pump manufacturer based on water-based performance tests. However, in actual field applications, fluid properties (e.g., viscosity, gas content) may significantly differ from laboratory test conditions, leading to deviations in pump performance. To address this, laboratory experiments were conducted (Figure 3). The acquired performance curves for the ESP under various viscosity conditions are presented in Figures 4–7.



FIGURE 3
The experimental setup.

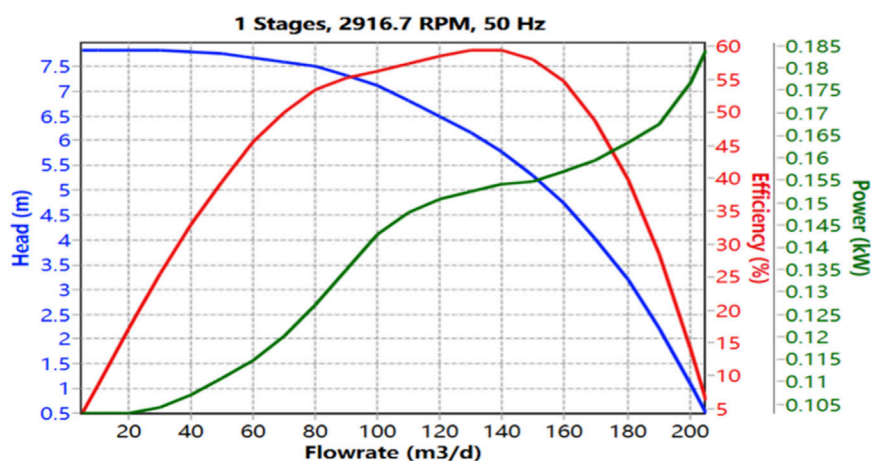


FIGURE 4
Performance curve of ESP.

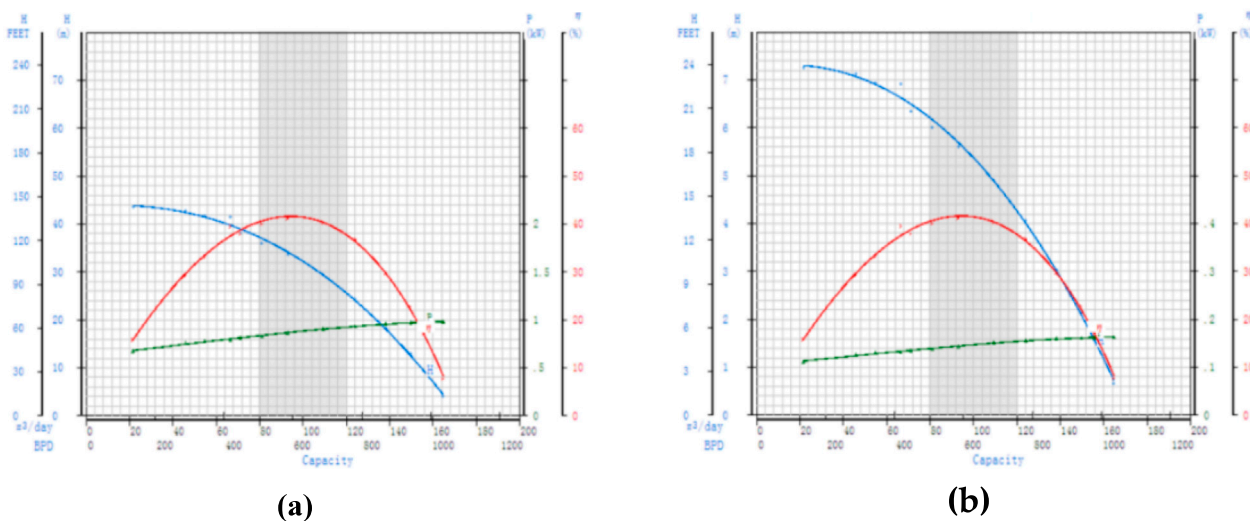
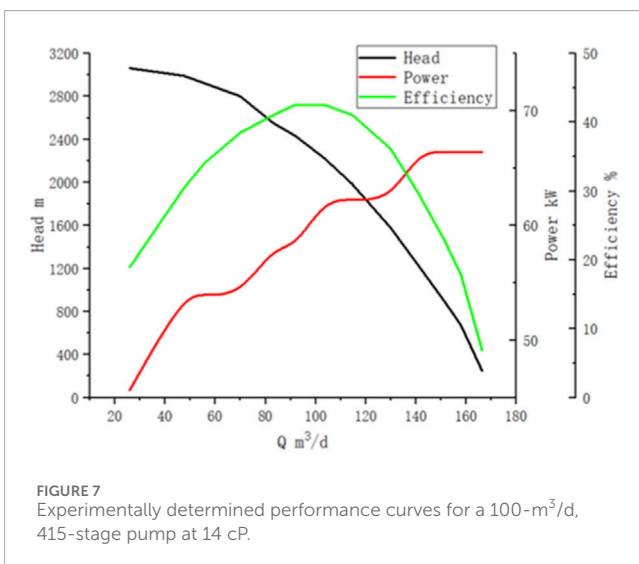
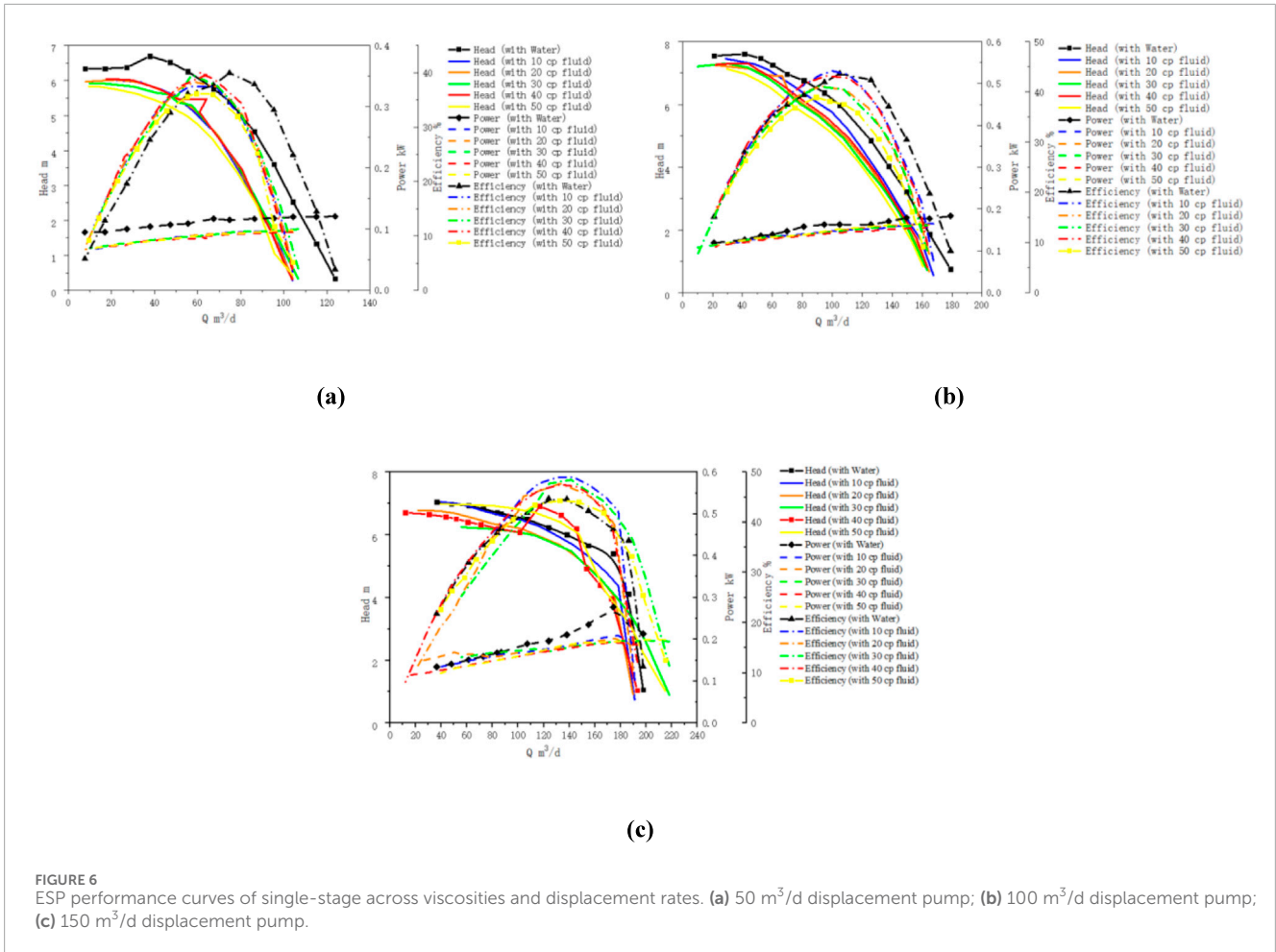


FIGURE 5
Performance curves with a rated displacement of 100 m³/d at 20 cP. (a) six stage pump; (b) single stage pump.



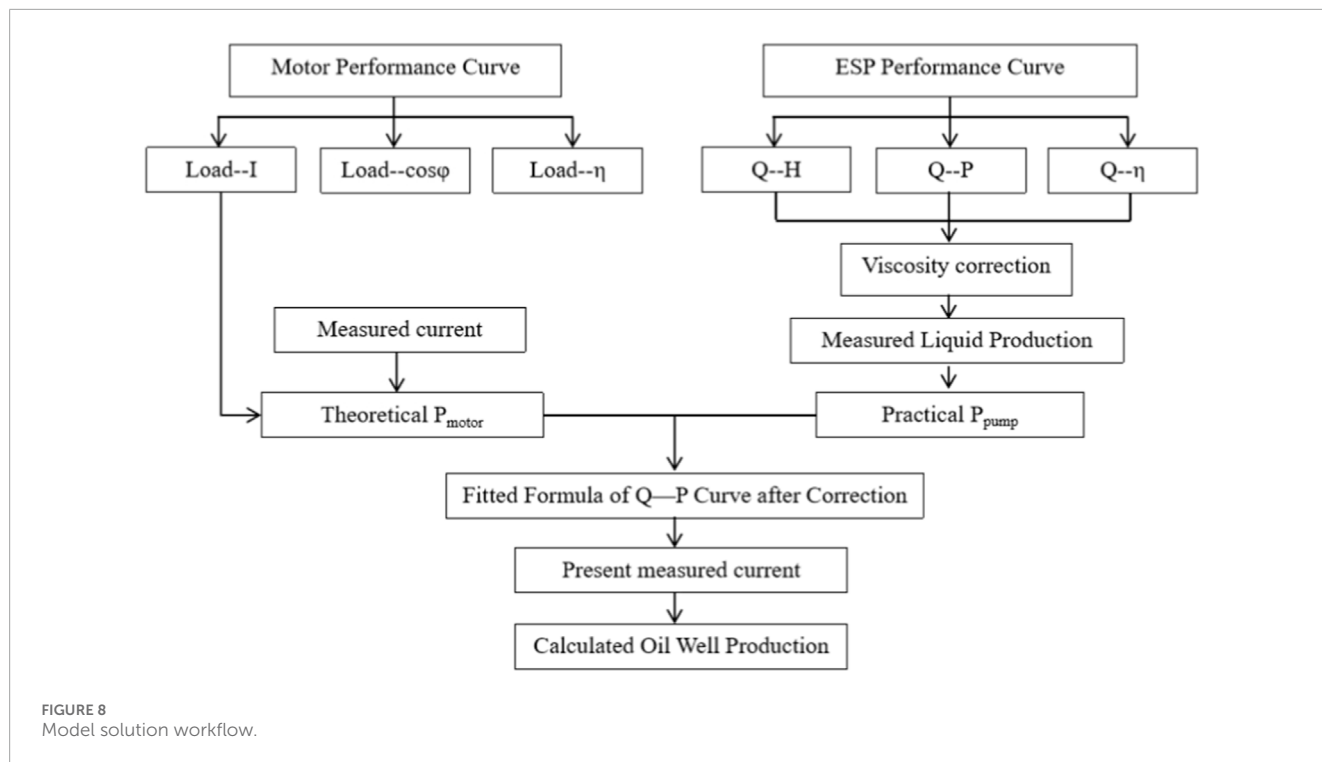
To address this, laboratory experiments were conducted using fluids with viscosities ranging from 10 to 50 cP to simulate real production environments. The experiments measured the performance parameters of the pump (head, efficiency, and power

consumption) at various flow rates under different viscosity conditions. The resulting data were used to construct corrected performance curves that account for viscous effects.

For motor performance curves (e.g., current vs. load rate), data were collected from surface current measurements and combined with the motor's nameplate parameters (e.g., rated power, voltage, current). The relationship between current and load rate was empirically derived to accurately estimate the motor's output power under actual operating conditions.

The pumps used in the experiment were provided by Block H, with rated displacements of 50, 100, and 150 m³/d, all identical models to those deployed in the field. During the tests, the viscosity of the fluid medium was adjusted by adding carboxymethyl cellulose (CMC) to clean water in proportional amounts to achieve target viscosities of 10, 20, 30, 40, and 50 cP.

The experimental procedure involved regulating the flow rate through the electric pump by adjusting a control valve. For each flow rate setting, corresponding head, power, and efficiency data were recorded after the system reached stable operating conditions. Data acquisition was performed via a computer interface, with each performance curve consisting of 13 or more data points to ensure accuracy and reliability. The comprehensive dataset enabled a detailed analysis of pump performance across the specified viscosity range.



The following figure presents the multistage and single-stage electric submersible pump (ESP) performance curves, generated by the computer-based control console, based on the acquired experimental data.

The experimentally measured performance curves provide a crucial foundation for the production estimation methodology. Compared to the standard performance curves provided by the manufacturer under clean water conditions, the acquired experimental data significantly reduce deviations caused by estimating pump behavior at varying viscosities using empirical formulas. Furthermore, this approach innovatively establishes a performance map specific to the electric submersible pump within the actual fluid viscosity range encountered in the oilfield.

As observed from the performance atlas, compared to clean water conditions, the three performance curves (head, efficiency, and power) of the 150 m³/d pump within the 10–50 cP viscosity range exhibit the following trends under constant frequency:

- Head decreases as viscosity increases.
- Efficiency decreases with increasing viscosity, yet all efficiency values across different viscosities remain higher than those in clean water.
- Power shows no significant variation with viscosity and remains lower than the power measured under clean water conditions.

For the 100 m³/d pump within the 10–50 cP viscosity range, the following trends were observed.

- Head decreases with increasing viscosity.
- Efficiency also decreases as viscosity rises, with the optimal efficiency point shifting to the left (toward lower flow rates).

- Power remains largely unaffected by viscosity changes and stays below the clean water power values.

For the 50 m³/d pump within the 10–50 cP viscosity range, the following trends were observed.

- Head values are consistently lower than those in clean water, but the sensitivity to fluid viscosity is relatively weak.
- Efficiency is lower than in clean water, with a leftward shift in the optimal efficiency point (more pronounced than that of the 100 m³/d pump), though no clear correlation with viscosity change is observed.
- Power shows minimal variation with viscosity and remains lower than the clean water power measurements.

The experimental results indicate that all impellers strictly follow the centrifugal pump affinity laws, with flow rate proportional to speed and head proportional to speed squared, and the 150 m³/d impeller showed optimal data stability. Notably, viscosity (10–50 cP) had no significant effect on flow rate (variation ≤3%), aligning with theory. However, the head response to viscosity differed: the 50 m³/d impeller performed best at 20–40 cP, whereas the 100 and 150 m³/d impellers suffered progressive head losses, greatest at 50 cP. This is attributable to increased energy dissipation at higher viscosities, to which larger-capacity impellers are more susceptible.

Experimental media were prepared with viscosities closely matching actual field fluid properties, and performance curve tests were conducted for the 50, 100, and 150 m³/d pumps within the 10–50 cP range. Experimental data within appropriate intervals were selected and interpolated to derive performance curves corresponding to the viscosities of different layers in Block H.

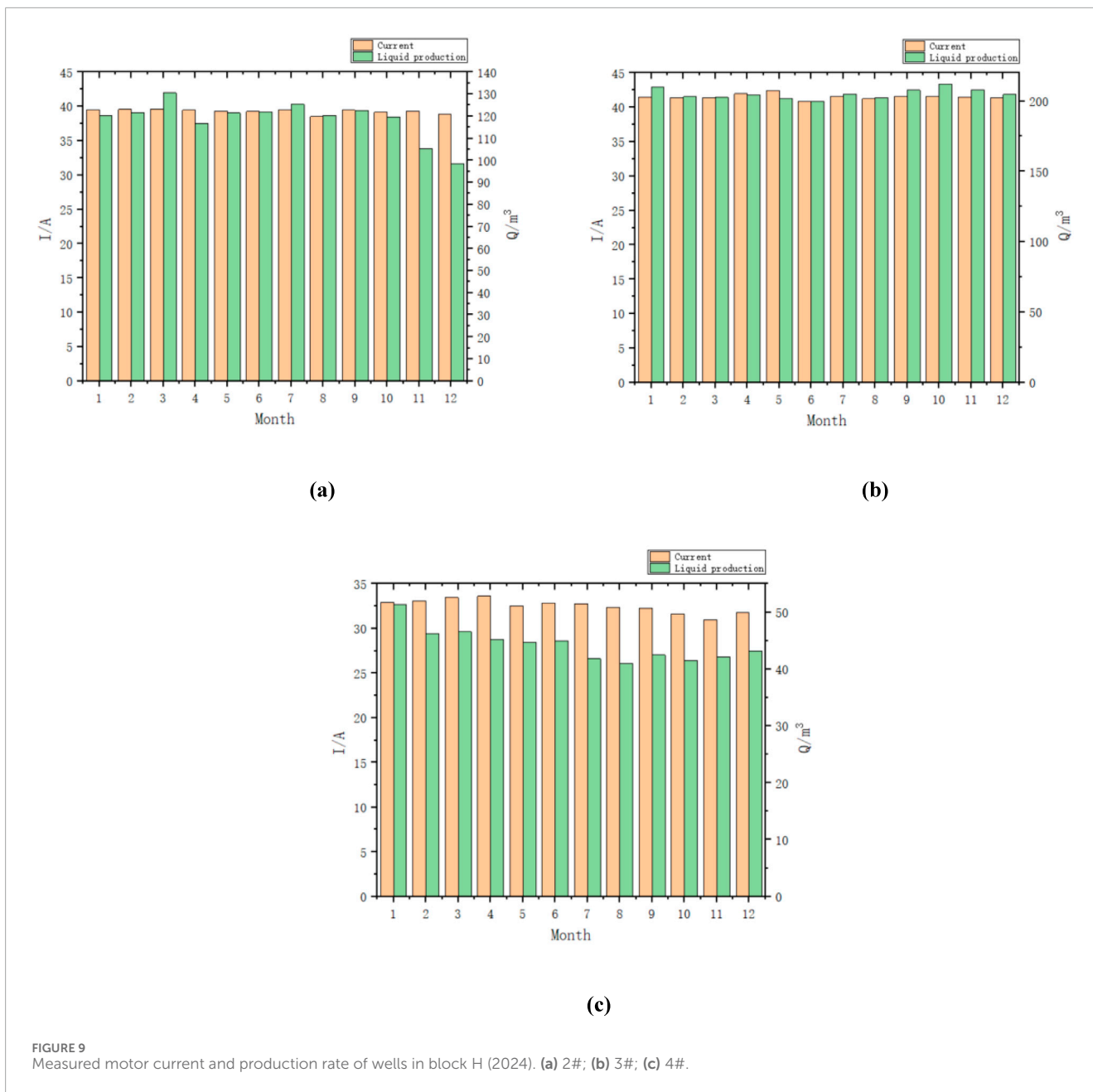


FIGURE 9 Measured motor current and production rate of wells in block H (2024). (a) 2#; (b) 3#; (c) 4#.

The performance curves and the subsequent model established in this study are based on laboratory testing with viscous liquid phases. Consequently, the current model is primarily validated and most accurate for conditions characterized by a low gas-volume fraction. While the model comprehensively accounts for the effects of fluid viscosity and density, the complex hydrodynamic behavior of multiphase flow (particularly high gas volume fraction conditions) is beyond the scope of this initial work. Extending the model to handle generalized multiphase flow will be a critical focus of future research.

4 Model solving

Based on the established model, the required inputs for solving the system include the motor performance curve, the pump P-Q

fitting curve, electrical current, historical production data, and the motor's rated specifications. The procedure for solving the model is out-lined as follows.

The overall workflow for solving the model is depicted in Figure 8. The specific steps are outlined as follows:

1. Correction of the Single-Stage Pump Performance Curve: Experimental data for the single-stage pump performance curve are corrected to account for the effects of high temperature and pressure conditions underground, which can reduce the viscosity of crude oil. Additionally, as the fluid transitions from the low-pressure suction inlet to the high-pressure discharge outlet, its density may vary due to compressibility. To mitigate the influence of disparities between surface tests and downhole

TABLE 2 Historical production data of Well #1 (January-February 2024).

Production date	Average current	Daily liquid production rate	Production date	Average current	Daily liquid production rate
2024/1/1	31.33	126	2024/2/1	31.15	121
2024/1/2	31.34	126	2024/2/2	31.07	121
2024/1/3	31.38	126	2024/2/3	31.19	122
2024/1/4	31.33	126	2024/2/4	31.35	122
2024/1/5	31.33	115	2024/2/5	31.33	122
2024/1/6	31.36	115	2024/2/6	31.30	122
2024/1/7	31.33	115	2024/2/7	31.24	122
2024/1/8	31.42	115	2024/2/8	31.32	122
2024/1/9	31.36	115	2024/2/9	31.31	122
2024/1/10	31.33	115	2024/2/10	31.35	122
2024/1/11	31.32	115	2024/2/11	31.3	122
2024/1/12	31.35	115	2024/2/12	31.29	122
2024/1/13	31.34	115	2024/2/13	31.27	122
2024/1/14	31.34	115	2024/2/14	31.26	122
2024/1/15	31.33	115	2024/2/15	31.28	122
2024/1/16	31.33	115	2024/2/16	31.31	122
2024/1/17	31.36	115	2024/2/17	31.32	122
2024/1/18	31.32	115	2024/2/18	31.33	122
2024/1/19	31.31	115	2024/2/19	31.34	122
2024/1/20	31.32	115	2024/2/20	697.60	122
2024/1/21	31.3	115	2024/2/21	1030.72	122
2024/1/22	31.32	115	2024/2/22	31.36	122
2024/1/23	31.3	115	2024/2/23	31.33	116
2024/1/24	31.18	121	2024/2/24	31.33	116
2024/1/25	31.22	121	2024/2/25	31.31	116
2024/1/26	31.19	121	2024/2/26	31.23	116
2024/1/27	31.13	121	2024/2/27	31.16	116
2024/1/28	31.09	121	2024/2/28	31.17	116
2024/1/29	31.23	121	2024/2/29	31.26	116
2024/1/30	31.32	121			
2024/1/31	31.15	121			

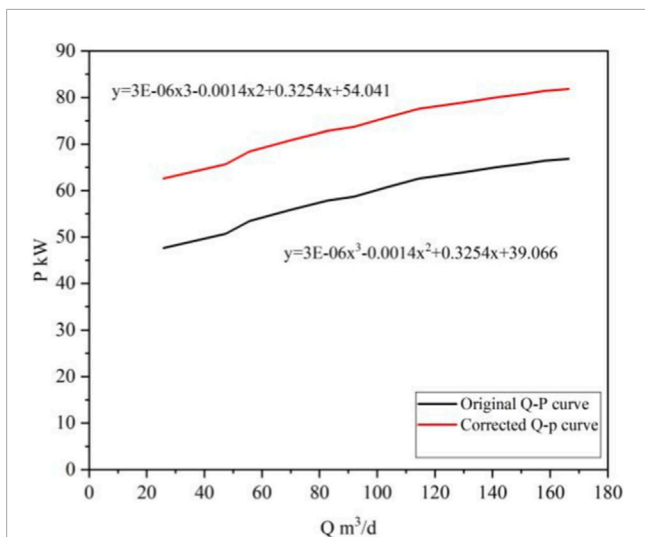


FIGURE 10
Calculated liquid production from electrical data using the corrected Q-P performance curve.

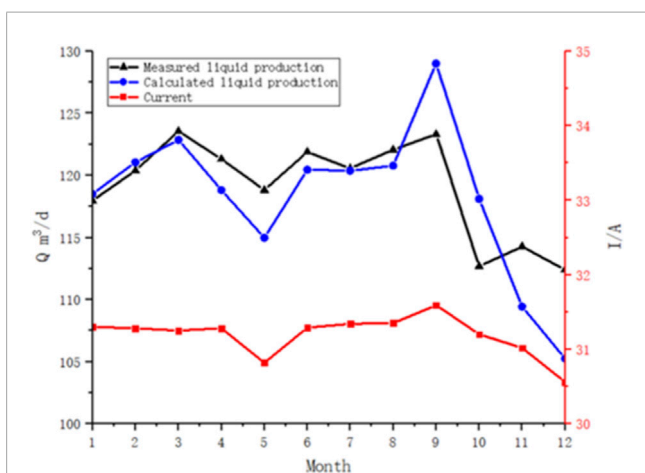


FIGURE 11
Comparison of measured and calculated production for #1 (2024).

conditions on fluid properties, correction factors $C_H = 1 - \left[(1 - C_{BEP-H}) \times \left(\frac{Q_W}{Q_{BEP-W}} \right)^{0.75} \right]$, $C_Q = (2.71)^{-0.165 \times (\log_{10} B)^{3.15}}$ and $C_\eta = B^{-(0.0547 \times B^{0.69})}$ are applied to the characteristics of the single-stage pump (Li et al., 2023; Yang et al., 2021; Xu et al., 2024; Bulgarelli et al., 2020) within the viscosity range of 10–50 cP. The corrected data are then interpolated to produce a curve that closely approximates the actual viscosity of the crude oil observed in the field. Following this, the characteristics of the individual pumps are summed according to the actual number of installed pump stages, generating the corresponding curve and fitting function.

- From the electrical parameter data in the database, the three-phase current values (I_A , I_B , I_C) are obtained, and the average current is calculated. This value is then compared to the motor’s rated current, and the corresponding motor load ratio is derived from the motor performance curve (current-load

ratio curve). This process yields the theoretical motor output power, P_{motor} .

- Power Calculation and Correction: Using production data, the corresponding power (P_{pump}) is determined from the fitting function of the pump P-Q performance curve. The difference between P_{motor} and P_{pump} is calculated, and this discrepancy is used to correct the Q-P curve within the performance curve.
- Prediction of Current Production: The current surface current data are used to estimate the new pump input power, P'_{motor} , which is then substituted into the adjusted P-Q characteristic function to predict the current liquid production rate.

5 Application and verification

The measured motor current and liquid production rate for each well in Block H (2024) are presented in Figure 9.

To validate the feasibility and accuracy of the aforementioned methodology, wells with varying displacement rates (50 m³/d, 100 m³/d, and 150 m³/d) and producing zones (each assigned a performance curve corresponding to zone-specific viscosity) were selected from the management area for performance evaluation. Electrical and production data spanning the entire year of 2024 were retrieved from the database. To streamline computation and enhance processing efficiency, the validation procedure was conducted monthly.

For instance, 1#, with a rated displacement of 100 m³/d and completed in the CI2 + 3 zone, is equipped with a 415-stage pump and a YQY138-type motor. The historical production data of Well #1 used for initial calibration is provided in Table 2. The motor’s rated parameters are 37 A, 2017 V, and 88 kW. Given a measured viscosity of 13.7 cP at 50 °C, the performance curve at 14 cP was interpolated using empirically derived curves at 10 cP and 20 cP.

For this well, the average current in January was 31.3 A, corresponding to 84.59% of the rated current. Based on the motor’s performance curve, the load factor was calculated to be 88.46%, resulting in a theoretical motor output power of 77.84 kW. Production data indicated an average liquid output of 117.968 m³/d in January. The corresponding power value derived from the original Q-P curve was 62.87 kW, resulting in the power discrepancy $\Delta P = 14.97 \text{ kW}$. This difference was used to adjust the performance curve, resulting in a revised P-Q fitting function: $y = 3E - 06x^3 - 0.0014x^2 + 0.3254x + 54.041$.

In the February dataset, current values from the 20th and 21st were identified as outliers due to abnormally high readings and excluded from the analysis. The recalculated average current for February was 31.28 A, representing 84.54% of the rated current. The motor performance curve indicated a load factor of 88.38%, corresponding to a theoretical motor output power of 77.77 kW.

The theoretical motor output power for February was applied to the adjusted P-Q curve derived in January, yielding a calculated production rate of 117.28 m³/d. This result was compared with the actual measured production for February, which was 120.37 m³/d. This calculation process, applying the corrected P-Q curve (Figure 10) to the current data, is repeated for prediction. The validation process was repeated for each month of 2024 using Well #1. A comparison between the actual

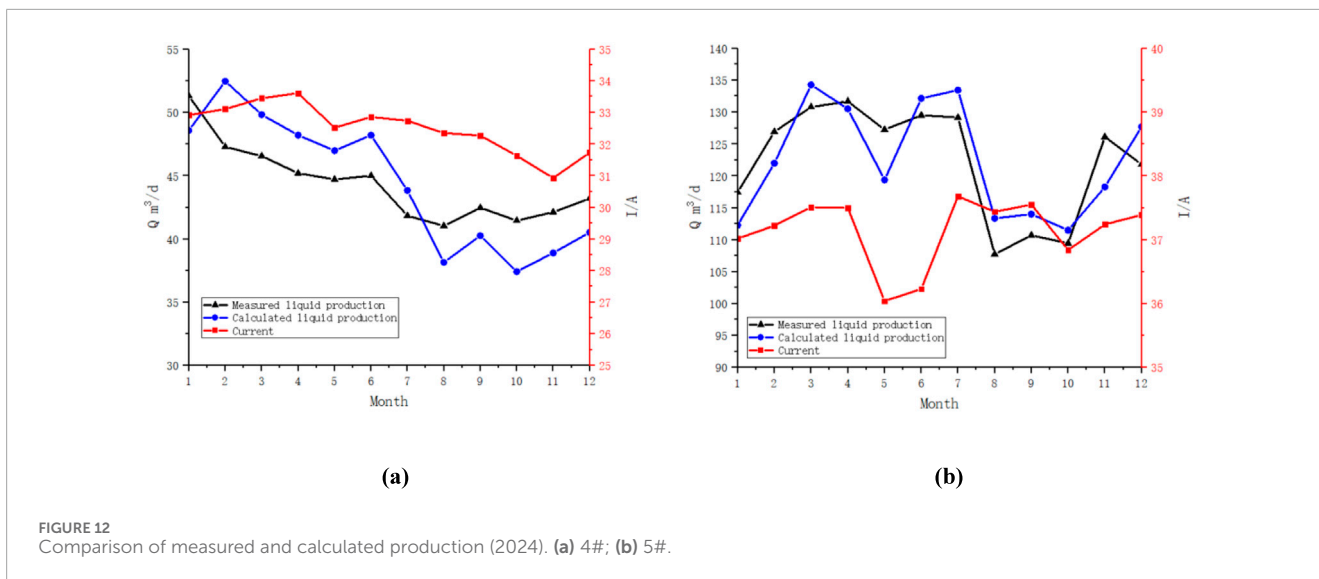


TABLE 3 Comparison of measured and calculated production for 2# (2024).

Well ID	Rated displacement (m ³ /d)	Motor model	Viscosity	Production date	Measured liquid production rate (m ³ /d)	Calculated liquid production rate (m ³ /d)	Deviation (m ³ /d)
2#	100	YQY114	16.01	2024-01	120.35	120.52	0.17
				2024-02	121.38	121.44	0.06
				2024-03	130.52	121.78	8.74
				2024-04	116.67	127.66	10.99
				2024-05	121.42	113.48	7.94
				2024-06	121.7	120.46	1.24
				2024-07	125.35	127.51	2.16
				2024-08	120.42	106.18	14.24
				2024-09	122.6	130.67	8.07
				2024-10	119.65	116.62	3.03
				2024-11	105.27	111.79	6.52
				2024-12	98.47	98.16	0.31

liquid production rates and the calculated values is shown in Figure 11.

The above method was used to verify the other four electric pump wells within Block H. The graphical comparisons for Wells #4 and #5 are shown in Figure 12, and the tabulated results for Wells #2 and #3 are provided in Tables 3, 4. A summary of extreme deviations across all wells is provided in Table 5, and a comprehensive error analysis is given in Table 6.

To more intuitively demonstrate the application of this method in each well, the following table has been compiled:

To provide a more comprehensive evaluation of the model's accuracy and facilitate comparison with other methods, root mean square error (RMSE) and monthly relative error (RE) were calculated for all test wells throughout 2024. As detailed in Table 6, the RMSE values for the five wells range from 3.17 to 6.99 m³/d. When expressed as a percentage of their respective rated displacements (50–150 m³/d), these RMSE figures correspond to relative root mean square errors between approximately 2% and 7%, indicating a consistently high level of prediction precision across different well capacities. The vast majority of monthly

TABLE 4 Comparison of measured and calculated production for 3# (2024).

Well ID	Rated displacement (m ³ /d)	Motor model	Viscosity	Production date	Measured liquid production rate (m ³ /d)	Calculated liquid production rate (m ³ /d)	Deviation (m ³ /d)
3#	150	YQY114	16.01	2024-01	209.68	210.82	1.14
				2024-02	203.7	207.55	4.48
				2024-03	202.65	202.04	0.61
				2024-04	204.5	215.35	10.85
				2024-05	201.97	214.47	12.5
				2024-06	199.76	193.57	6.19
				2024-07	204.9	212.49	7.59
				2024-08	202.29	198.9	3.39
				2024-09	207.77	209.71	1.94
				2024-10	212	207.5	4.5
				2024-11	208	209.31	1.31
				2024-12	204.73	205.89	1.16

TABLE 5 Comparison of measured and calculated production rates for 3# (2024).

Rated displacement (m ³ /d)	Well ID	Maximum deviation (m ³ /d)	Minimum deviation (m ³ /d)
50	4#	7.19	1.99
100	1#	5.71	0.19
	2#	14.24	0.06
	5#	7.87	1.18
150	3#	12.5	0.6

relative errors are below 10%, with only a few isolated instances exceeding this threshold (e.g., a maximum of 11.82% in Well 2# and 10.98% in Well 4#). These results demonstrate that the model maintains robust accuracy under varied production conditions.

6 Conclusions and recommendations

1. This study experimentally quantified the impact of fluid properties on ESP performance by establishing performance maps under various viscosity and density conditions. Compared to manufacturer-provided clean-water curves, the data more accurately represent pump behavior in actual downhole fluids. The results reveal a non-uniform

performance response to viscosity. For instance, high-flow-rate impellers exhibit significant head loss. In contrast, some models show an optimal efficiency window at medium viscosities. These validated performance maps provide a reliable reference for production estimation, pump selection, and field diagnostics.

2. This study successfully developed and validated a production metering model for ESP wells based on the energy balance principle, where the pump input power is equated to the motor output power. The model was solved by integrating motor and pump performance curves with actual current data from Block H. Crucially, the pump performance curves were refined using experimental data obtained under varying viscosity conditions, moving beyond the limitations of standard water-based curves. This enhanced model provides a reliable

TABLE 6 The relative error and root mean square error of five wells (each month of 2024).

Well ID	Root mean square error	Relative error (%)	Well ID	Root mean square error	Relative error (%)	Well ID	Root mean square error	Relative error (%)
1#	3.68	0.46%	2#	6.99	0.13%	3#	6.79	5.31%
		0.56%			0.05%			2.20%
		0.57%			6.69%			0.30%
		2.05%			9.43%			5.31%
		3.22%			6.54%			6.19%
		1.17%			1.02%			3.10%
		0.16%			1.72%			3.70%
		1.06%			11.82%			1.68%
		4.63%			6.58%			0.93%
		4.82%			2.52%			2.12%
		4.24%			6.20%			0.63%
		6.36%			0.32%			0.57%
4#	3.17	5.34%	5#	4.96	4.40%			
		10.98%			3.89%			
		7.05%			2.65%			
		6.66%			0.90%			
		5.08%			6.18%			
		7.13%			2.05%			
		4.76%			3.31%			
		7.02%			5.21%			
		5.20%			3.00%			
		9.72%			1.85%			
		7.64%			6.22%			
		6.20%			4.85%			

theoretical foundation for improving intelligent production management in ESP wells, enabling more accurate production monitoring without downhole sensors.

3. The validation results demonstrate that the maximum prediction error in liquid production rates across all three types of ESP wells remains within 15% of their rated displacement, confirming the method’s feasibility and accuracy for the low-gas-viscous fluid conditions under which it was calibrated.

4. For wells exhibiting significant calculation discrepancies, the errors are likely attributable to two primary factors: the compatibility between viscous drag and impeller flow passage design, or suboptimal data acquisition quality. To enhance model robustness, it is strongly recommended to implement rigorous data cleaning protocols.

5. This study successfully establishes a cost-effective and accurate digital metering solution for ESP wells producing under low-gas-viscous fluid conditions. Building upon this foundation,

a natural and valuable extension of this research would be to incorporate multiphase flow dynamics, thereby extending its applicability to a wider range of production scenarios.

Data availability statement

The original contributions presented in the study are included in the article/supplementary material, further inquiries can be directed to the corresponding author.

Author contributions

JY: Validation, Methodology, Writing – original draft, Investigation, Software, Visualization, Formal Analysis. RZ: Conceptualization, Formal Analysis, Writing – review and editing. GM: Methodology, Writing – review and editing, Formal Analysis.

Funding

The author(s) declared that financial support was not received for this work and/or its publication.

References

- Al Qahtani, A., Al Qahtani, M., and Al Qahtani, B. (2020). "Development of a novel solution for multiphase flow metering in ESP-lifted wells," in *Proceedings of the Abu Dhabi international petroleum exhibition and conference* (Abu Dhabi, UAE). doi:10.2118/203480-MS
- Amin, A. (2015). "Evaluation of commercially available virtual flow meters (VFMs)," in *Proceedings of the offshore technology conference* (Houston, TX, USA: Offshore Technology Conference). doi:10.4043/25764-MS
- Barrios, L., Scott, S., Rivera, R., and Prado, M. (2012). "Surveillance models of large-scale ESP performance with high viscosity fluids and gas," in *Proceedings of the SPE international production and operations conference and exhibition* (Richardson, TX, USA: Doha), 14–16. doi:10.2118/152217-MS
- Batzle, M., and Wang, Z. (2019). Multiphase flow modeling for electric submersible pump performance prediction. *SPE J.* 24 (4), 1632–1645. doi:10.2118/194183-PA
- Bikmukhametov, T., and Jaschke, J. (2019). First principles and machine learning virtual flow metering: a literature review. *J. Pet. Sci. Eng.* 184, 106487. doi:10.1016/j.petrol.2019.106487
- Bulgarelli, N. A. V., Biazussi, J. L., Verde, W. M., Perles, C. E., Castro, M. S., and Bannwart, A. C. (2020). Experimental investigation on the performance of Electrical Submersible Pump (ESP) operating with unstable water/oil emulsions. *J. Petroleum Sci. Eng.* 195, 107900. doi:10.1016/j.petrol.2020.107900
- Caicedo, S., and Montoya, C. (2012). "Estimating flow rates based on ESP Down hole sensor data," in *Proceedings of the SPE Kuwait international petroleum conference and exhibition, Kuwait city, Kuwait, 10–12 December 2012* (Richardson, TX, USA: Society of Petroleum Engineers (SPE)).
- Camilleri, L. A. P., Banciu, T., and Ditoiu, G. (2010). "First installation of 5 ESPs offshore romania—A case study and lessons learned," in *Proceedings of the SPE intelligent energy conference and exhibition* (Utrecht, Netherlands). doi:10.2118/127593-MS
- Camilleri, L., El Gindy, M., Rusakov, A., and Adoghe, S. (2015). "Converting ESP real-time data to flow rate and reservoir information for a remote oil well," in *Proceedings of the SPE Middle East intelligent oil and gas conference and exhibition, Abu Dhabi, UAE, 15–16 September 2015* (Richardson, TX, USA: Society of Petroleum Engineers SPE). doi:10.2118/176780-MS
- Camilleri, L., El Gindy, M., and Rusakov, A. (2016). "Providing accurate ESP flow rate measurement in the absence of a test separator," in *Proceedings of the SPE annual technical conference and exhibition, Dubai* (Richardson, TX, USA: UAE), 26–28. doi:10.2118/181663-MS
- Del Pino, J. J., Martin, J. L., Vargas, H., Maldonado, J. S., Rubiano, E., Núñez, W., et al. (2017). "Installation of electric submersible pump as artificial lift method in low flow rate Wells, a case history," in *Proceedings of the SPE electric submersible pump symposium, the woodlands, TX, USA, 24–28 April 2017; SPE* (Richardson, TX, USA). doi:10.2118/185155-MS
- Gryzlov, A., Mironova, L., Safonov, S., and Arsalan, M. (2021). "Artificial intelligence and data analytics for virtual flow metering," in *Proceedings of the SPE Middle East oil and gas show and conference* (Richardson, TX, USA). doi:10.2118/204662-MS
- Li, Y., Gong, J., Chen, L., Liu, J. R., Li, B. Y., and Luo, M. L. (2018). Application of On-Line production metering method for electric pump Wells with capillary piezometry in offshore oilfields. *Oil Drill. Prod. Technol.* 40 (6), 829–834. doi:10.13639/j.odpt.2018.06.025
- Li, W. W., Fu, P., and Huang, B. (2023). Downhole flow measurement system for submersible electric pump. *Pet. Field Eng.* (1D), 46. doi:10.16621/j.cnki.issn1001-0599.2023.01D.46
- Liu, Y. H., and Chen, D. C. (2020). Numerical simulation and experiment of multiphase flow in oil-gas lifting system. *Acta Pet. Sin.* 41 (3), 385–393.
- Liu, Y., and Zhang, L. (2022). Fluid immiscibility and evolution in subduction zones. *Acta Geol. Sin.* 96, 4101–4130. doi:10.1111/1755-6724.15000
- Morrison, G., Pirospanah, S., Kirland, K., Scott, S. L., and Barrios, L. J. (2014). "Performance evaluation of a multiphase electric submersible pump," in *Proceedings of the offshore technology conference* (Richardson, TX, USA: OTC). doi:10.4043/25080-MS
- Peng, R., Ju, Y., Gao, F., and Xie, H. (2014). Energy analysis on damage of coal under cyclical triaxial loading and unloading conditions. *J. China Univ. Min. Technol.* 43, 1–6. doi:10.13225/j.cnki.jccs.2013.2010
- Reiners, P. W., Barton, I., Barton, M. D., Hirt, W. C., Kirk, J., Krantz, R. W., et al. (2019). Evolution of the paradox basin subsurface fluid-flow system and paleofluid-rock reaction products. *Geol. Soc. Am. Abstr. Prog.* 51, 335015. doi:10.1130/abs/2019am-335015
- Tangren, R. F., Dodge, C. H., and Seifert, H. S. (1949). Compressibility effects in two-phase flow. *J. Appl. Phys.* 20, 637–645. doi:10.1063/1.1698449
- Varón, M. P., Biazussi, J. L., Bannwart, A. C., Monte Verde, W., and Sassim, N. (2013). "Study of an electrical submersible pump (ESP) as flow meter," in *Proceedings*

Conflict of interest

The author(s) declared that this work was conducted in the absence of any commercial or financial relationships that could be construed as a potential conflict of interest.

Generative AI statement

The author(s) declared that generative AI was not used in the creation of this manuscript.

Any alternative text (alt text) provided alongside figures in this article has been generated by Frontiers with the support of artificial intelligence and reasonable efforts have been made to ensure accuracy, including review by the authors wherever possible. If you identify any issues, please contact us.

Publisher's note

All claims expressed in this article are solely those of the authors and do not necessarily represent those of their affiliated organizations, or those of the publisher, the editors and the reviewers. Any product that may be evaluated in this article, or claim that may be made by its manufacturer, is not guaranteed or endorsed by the publisher.

of the SPE artificial lift conference—americas, cartagena, Colombia, 21–22. doi:10.2118/165065-MS

Xu, H. F., Wu, T. S., Sun, G. B., Li, Z. H., and Chen, B. (2024). Deep learning-based virtual flow metering system for electric submersible pump Wells. *Pet. Eng. Technol.* (4), 70–74.

Xue, Y., He, X., Song, D., Li, Z., Khan, M., Zhong, T., et al. (2024). Energy evolution and structural health monitoring of coal under different failure modes: an

experimental study. *Int. J. Min. Metall. Mater.* 31, 917–928. doi:10.1007/s12613-023-2769-4

Yang, J. Z., Feng, G., Wang, Q. H., Zou, H. L., and Ma, D. (2021). Deep learning based dynamic prediction model of ESP well production. *Oil Drill. and Prod. Technol.* 43 (4), 489–496. doi:10.13639/j.odpt.2021.04.012

Zhou, D. S. (2017). *Optimization design technology for electric submersible pump production systems*. Beijing, China: Petroleum Industry Press.